

AD-A247 628



## REPORT DOCUMENTATION PAGE

②

23 SECURITY CLASSIFICATION AUTHORITY			1b RESTRICTIVE MARKINGS			
2b DECLASSIFICATION / DOWNGRADING SCHEDULE			3 DISTRIBUTION / AVAILABILITY OF REPORT This document has been approved for public release and sale; its distribution is unlimited.			
4 PERFORMING ORGANIZATION REPORT NUMBER(S) 12			5 MONITORING ORGANIZATION REPORT NUMBER(S)			
6a NAME OF PERFORMING ORGANIZATION NIST		6b OFFICE SYMBOL (If applicable)		7a. NAME OF MONITORING ORGANIZATION ONR		
6c ADDRESS (City, State, and ZIP Code) A329, Materials Building Gaithersburg, MD 20899		7b ADDRESS (City, State, and ZIP Code) Code 1131 800 N. Quincy Street Arlington, VA 22217-5000				
8a. NAME OF FUNDING / SPONSORING ORGANIZATION ONR		8b. OFFICE SYMBOL (If applicable)		9. PROCUREMENT INSTRUMENT IDENTIFICATION NUMBER N00014-90-F-0011		
8c. ADDRESS (City, State, and ZIP Code)		10 SOURCE OF FUNDING NUMBERS				
		PROGRAM ELEMENT NO		PROJECT NO	TASK NO	
					WORK UNIT NO	
11 TITLE (Include Security Classification)						
12 PERSONAL AUTHOR(S) A. Feldman, E.N. Farabaugh, L.H. Robins, D. Shechtman						
13a. TYPE OF REPORT Interim		13b. TIME COVERED FROM TO		14 DATE OF REPORT (Year, Month, Day) 1992-Feb-20		
				15. PAGE COUNT 19		
16 SUPPLEMENTARY NOTATION						
17 COSATI CODES			18. SUBJECT TERMS (Continue on reverse if necessary and identify by block number)			
FIELD	GROUP	SUB-GROUP	This document has been approved for public release and sale: its distribution is unlimited.			
19 ABSTRACT (Continue on reverse if necessary and identify by block number)						
CVD diamond, which is mainly polycrystalline, exhibits several materials problems that limit its optical transmission, such as scattering due to large surface roughness and absorption due to defects, nondiamond carbon phases, and impurities. Optical spectroscopy, Raman spectroscopy, cathodoluminescence imaging and spectroscopy, and high resolution electron microscopy are used to examine the defects in the material; however, a relationship between observed defects and optical absorption is not always evident. New polishing methods are promising an ability to produce smooth surfaces in reasonable polishing times.						
20 DISTRIBUTION / AVAILABILITY OF ABSTRACT <input checked="" type="checkbox"/> UNCLASSIFIED/UNLIMITED <input type="checkbox"/> SAME AS RPT <input type="checkbox"/> DTIC USERS			21 ABSTRACT SECURITY CLASSIFICATION Unclassified			
22a NAME OF RESPONSIBLE INDIVIDUAL			22b TELEPHONE (Include Area Code)		22c. OFFICE SYMBOL	

OFFICE OF NAVAL RESEARCH

Contract N00014-90-F-0011

R&T Project No. IRMT 025

TECHNICAL REPORT No. 12

DIAMOND AS AN OPTICAL MATERIALS

A. Feldman, E.N. Farabaugh, L.H. Robins, and D. Shechtman\*

submitted to

*Characterization of Optical Materials*

National Institute of Standards and Technology

Ceramics Division

Gaithersburg, MD 20899

February 20, 1992

Accession For	
NTIS	CRA&I <input checked="" type="checkbox"/>
DTIC	TAB <input type="checkbox"/>
Unannounced	<input type="checkbox"/>
Justification	
By	
Distribution/	
Availability Codes	
Dist	Avail. and/or Special
A-1	

Reproduction in whole or in part is permitted for  
any purpose of the United States Government

This document has been approved for public release  
and sale; its distribution is unlimited

\*Visiting scientist at the Johns Hopkins University and at NIST from the Technion,  
Israel.

92 3 18 038

92-07005



## DIAMOND AS AN OPTICAL MATERIAL(a,b)

Albert Feldman, L.H. Robins, E.N. Farabaugh  
Ceramics Division, Materials Science and Engineering Laboratory  
National Institute of Standards and Technology  
Technology Administration  
U.S. Department of Commerce

Gaithersburg, MD 20899

D. Shechtman(c)  
Technion, Haifa (Israel)

### Table of Contents

1. INTRODUCTION
2. DISCUSSION
  - 2.1 Deposition Methods
  - 2.2 Optical Properties of CVD Diamond
  - 2.3 Defects in CVD Diamond
  - 2.4 Polishing CVD Diamond
  - 2.5 X-ray Window
3. CONCLUSION
4. ACKNOWLEDGEMENT
5. REFERENCES

### 1. INTRODUCTION

The high transmissivity of perfect diamond over extensive regions of the electromagnetic spectrum, in combination with diamond's great hardness, large abrasion resistance, high thermal conductivity, and chemical inertness make diamond a highly desirable optical material. Until recently, the high cost and small dimensions of optical quality diamond have limited the use of diamond to a few specialized optical applications; the best optical quality diamond, type IIa diamond, still comes from natural sources. However, new chemical vapor deposition (CVD) processes have the potential to make available inexpensive bulk diamonds of large dimensions and thin film diamond to cover large areas, thus making possible the widespread use of diamond optics and optical coatings [1,2,3]. X-ray windows of CVD diamond are already commercially available [4]. Anticipated optical applications include infrared windows and domes, high power laser windows, and membranes for x-ray lithography [5]. Other possible applications include electroluminescent devices [6], lasers [7], and optical switches [8].

-----  
(a) This is a contribution of the National Institute of Standards and Technology. Not subject to copyright.

(b) This work was supported in part by the Office of Naval Research.

(c) Visiting scientist at the Johns Hopkins University and at the National Institute of Standards and Technology

This article focuses principally on the status of CVD diamond as an optically transparent material. CVD diamond, which is mainly polycrystalline, exhibits several materials problems that limit its optical transmission, such as scattering due to large surface roughness and absorption due to defects, nondiamond carbon phases, and impurities. New polishing methods have the potential for producing smooth surfaces in reasonable polishing times; however, work on surface figure, to our knowledge, has not yet been addressed. While intrinsic multiphonon processes limit the transmissivity of all diamond between 2.5 and 6.5  $\mu\text{m}$ , CVD diamond usually contains high densities of lattice defects causing normally forbidden single phonon absorption processes to occur between 7.5 to 12  $\mu\text{m}$ . In addition, free carrier absorption in CVD diamond has also been reported. While diamond windows less than 10  $\mu\text{m}$  thick can be made transmissive to visible and ultraviolet radiation, thicker components scatter excessively and show absorption due to defects. Raman spectroscopy is the principal method for observing the presence of nondiamond carbon phases in CVD diamond.

An important method for examining point defects in CVD diamond is cathodoluminescence spectroscopy. When conducted in a scanning electron microscope (SEM), cathodoluminescence images can be generated that provide information about the spatial distribution of luminescent defects on a submicrometer scale. However, the relationship between the observed cathodoluminescence and defect induced optical absorption has not yet been established. Luminescence has been the basis for diamond devices that emit optical radiation. Lasers and electroluminescent devices have been made but the quantum efficiency at present is too small for these devices to be of practical use.

A powerful method for observing defects close to the atomic level is high resolution transmission electron microscopy. Here again, the relationship between observed defects and optical absorption has not been correlated.

Continuing research is improving the optical quality of CVD diamond. Recently, novel methods for producing single crystal (non-CVD methods) or near single crystal diamond have been reported. When fully developed, these methods could make available large optics of single crystal diamond.

High deposition temperature, large thermal expansion mismatch, and poor adhesion now limit the use of CVD diamond as a hard coating material. To overcome some of these difficulties, a method has been developed to place a diamond coating on ZnSe by bonding the coating to the substrate with a chalcogenide glass layer [9].

## 2. DISCUSSION

### 2.1 Deposition Methods

Several deposition methods are being used to deposit diamond by CVD. High quality polycrystalline diamond has been made by hot filament CVD [3], microwave plasma CVD [10], DC plasma torch [11], radio frequency plasma torch [12,13], microwave plasma torch [14], and oxyacetylene torch [15]. Figure 1 shows SEM images of diamond films showing typical surface

morphologies [16]. The morphologies observed are common to all of the deposition methods. The films were grown on silicon wafer substrates in a hot filament reactor under different deposition conditions.

Except for the oxyacetylene torch method, the charge gas for producing diamond is hydrogen mixed with a hydrocarbon such as methane, acetylene, methyl alcohol, ethyl alcohol, or acetone [17]. The hydrogen fraction in the feed gas is almost always greater than 90 per cent. The quality of the diamond usually improves with increasing hydrogen fraction in the feed gas. It is also found that oxygen added to the charge gas improves the diamond quality [18]. Carbon monoxide mixed with hydrogen has also been used [19]. In the plasma torch methods, argon is sometimes used as a sheath gas. In the case of the oxyacetylene torch, only acetylene and oxygen comprise the charge gas. In this case, deposition is carried out in the reducing part of an oxygen-poor torch flame.

Substrate temperatures during deposition are usually maintained at a constant temperature in the range 600 to 1000 °C. Depositions have been done at temperatures below 400 °C [20]; however, the growth rates are low and the quality of the diamond, as determined by Raman spectroscopy, is poor. Recently, depositions by the oxyacetylene torch method at substrate temperatures up to 1600 °C have resulted in the growth of single crystal diamonds at high growth rates [21]. The method appears very promising for producing boule-sized single crystal diamonds of high optical quality.

A creative method for producing nearly single crystal diamonds layers over large areas has been developed recently [22]. Selective area etching was used to produce an array of etch pits of a well defined pyramidal shape in a single crystal silicon substrate. A slurry containing single crystal diamond particles of a matching pyramidal shape was applied to the surface of the substrate and then removed. Diamond particles that had been left behind were embedded in each of the etch pits. These particles were crystallographically oriented to within several degrees. When the substrate was placed in a CVD reactor, the diamond particles acted as seeds for diamond growth, resulting in a continuous diamond film that was nearly a single crystal.

There have been two reports of single crystal diamond nucleation on single crystal copper substrates. Both methods rely on the lack of solubility of carbon in copper. In one experiment [23], carbon ions were implanted into a single crystal copper substrate at an elevated temperature. A transmission electron microscope diffraction pattern indicated that a single crystal diamond layer had formed on the surface of the copper.

In the other experiment, carbon ions were implanted into single crystal copper substrates at room temperature [24]. The surface of the specimen was then exposed to high power radiation from an excimer laser. The laser pulse energy was chosen to cause the surface of the copper substrate to melt and then to refreeze rapidly. During refreezing of the copper, the carbon atoms were expelled and forced to the surface, precipitating on the surface as a diamond layer.

A halogen-assisted CVD method has recently been discovered for producing diamond [25]; however, this research is in an early stage and claims for

good quality diamond films made by this method have not yet been reported.

## 2.2 Optical Properties of CVD Diamond.

Many of the projected optical applications of CVD diamond are based on the known intrinsic properties of diamond. The intrinsic absorption mechanisms of diamond are due to interband transitions of electrons across the fundamental electronic energy gap at 5.45 eV, and to multiphonon generation in the infrared between 2.5 and 6.5  $\mu\text{m}$ . Generally, absorption due to 2-phonon and 3-phonon generation predominates; higher order phonon generation has significantly decreased probability. Absorption due to generation of single phonons is forbidden because of crystal symmetry. Thus, perfect diamond is transparent between 225 nm in the ultraviolet and 2.5  $\mu\text{m}$  in the infrared, and from 6.5  $\mu\text{m}$  in the infrared to zero frequency (DC). Because the absorption process in the infrared between 2.5 and 6.5  $\mu\text{m}$  is of second order and higher, the absorption coefficients are small so that thin diamond films may transmit adequately for many infrared applications in this wavelength range.

CVD diamond is not yet of the quality of the best natural single crystals because of the high density of defects in the material [26]. Several types of defects are present. Lattice defects, such as grain boundaries, twin boundaries, stacking faults, and dislocations, break the crystal symmetry of the diamond lattice resulting in absorption due to generation of single phonons. Thus, absorption by single phonon generation in CVD diamond has been observed at wavelengths longer than 6.5  $\mu\text{m}$ . Many of the principal features in the diamond phonon spectrum have been identified in these transmission spectra [26].

Impurities can produce electronic states within the electronic band gap or can lead to local vibrational modes resulting in unwanted absorption. Nitrogen is known to significantly limit the transmission of diamond in the ultraviolet and is responsible for absorption features in the infrared [27]. Hydrogen in combination with carbon produces a C-H stretch absorption feature in the infrared near 2800  $\text{cm}^{-1}$  [26,28-35]. Other spectral features due to hydrogen have been observed in bulk diamond and may be present in CVD diamond [36].

Figure 2 shows an infrared absorption spectrum of a CVD diamond polycrystalline specimen prepared by microwave plasma CVD showing the one phonon, two phonon, and three phonon absorption regions and absorption due to a C-H stretch mode [26].

CVD diamond usually contains nondiamond carbon phases that induce absorption, especially in the visible and ultraviolet. Figure 3 shows the absorption coefficient of CVD diamond and of type IIa diamond in the vicinity of the indirect absorption edge near 5.5 eV [37]. The higher absorption coefficient and the absorption tail extending to lower photon energies for the films is believed due to disordered carbon.

The presence of nondiamond phases of carbon is usually detected by Raman spectroscopy. The Raman spectrum of pure diamond consists of a single peak located at 1332  $\text{cm}^{-1}$  wavenumber shift. CVD diamond usually exhibits an additional broad peak near 1500  $\text{cm}^{-1}$  that is attributed to the nondiamond carbon phases. The sizes of the two peaks (after subtraction for any

luminescence background signal) can be used as a qualitative measure of the diamond quality. Figure 4 shows a Raman spectrum typical of CVD diamond.

Recent experiments have shown that diamond can be made highly transmissive in the far infrared. Attenuation of the optical signal was attributed both to free carrier absorption and to optical scatter [35].

### 2.3 Defects in CVD Diamond

Defects such as nondiamond phases of carbon, point defects, impurities, lattice imperfections, etc., are an important factor in the optical performance of CVD diamond. Cathodoluminescence imaging and spectroscopy provide a means for examining point defects and impurities in diamond on a microscopic scale [38]. In this method, the specimen is placed in a scanning electron microscope and the optical radiation emitted by the specimen is collected by a photodetector. The optical signal arises when valence band electrons are excited above the fundamental energy gap of the diamond into the conduction band by the energetic electron beam ( $>10$  kV) of the SEM. The electrons in the conduction band can decay to defect states within the band gap. The electrons may lose energy from these defect states by emitting optical radiation whose spectral features are characteristic of the defect center.

The cathodoluminescence provides an optical image of the specimen as the electron beam scans over the specimen. This image can be compared to the secondary electron image customary observed with the SEM. Figure 5 shows a cathodoluminescence image and a secondary electron SEM image of diamond particles deposited by CVD. The cathodoluminescence image provides information regarding the distribution of luminescent defects in the diamond. However, the interpretation of the image in terms of defect densities is not necessarily straightforward because the intensity of the luminescence from a particular defect species depends not only on the number density of that species but also on the densities of other species that give rise to competing decay processes.

By a spectral analysis of the cathodoluminescence, one can deduce the nature of the defect centers. This identification is based on a large body of work in which the luminescence spectra of many defects have been identified. Figure 6 is the cathodoluminescence spectrum of a diamond film that shows several spectral features often observed in CVD diamond. These features have been associated with particular defects: a sharp line at 1.68 eV believed to be due to a silicon impurity introduced during deposition (this feature is identical to the luminescence line frequently observed at  $5890\text{ cm}^{-1}$  in the Raman spectrum); a line at 2.156 eV and an associated vibronic band centered near 2 eV, due to a nitrogen-vacancy (N-V) complex; a line at 2.326 eV due to a different N-V complex; and, a broad violet band centered at 2.85 eV, due to a dislocation related defect. A line at 3.188 eV due to a nitrogen interstitial-carbon complex has also been observed in some CVD diamond films.

High resolution electron microscopy is a powerful tool for examining defects in CVD diamond at the lattice scale [39]. Figure 7 shows a high resolution electron micrograph of CVD diamond with a  $\langle 110 \rangle$  orientation showing a large number of twinning defects. The film was prepared by the microwave plasma technique and thinned for examination in the electron microscope. All

of the observed twins retain a crystallographical relationship to each other. All arrows point to misfit twin boundaries, which are described below. The hollow arrows also point along local growth directions.

A preferred nucleation site for diamond growth is a location where five twins come together to a point. This structure is called a twin quintuplet. Figure 8 is an enlarged view of a twin quintuplet and several other twins. A coherent twin boundary occurs when  $\{111\}$  planes of adjacent twins are in coincidence and this is evident for most of the twin boundaries in the figure.

Because the angle between  $\{111\}$  planes in a crystal twin is  $70.5^\circ$ , a  $7.5^\circ$  angular mismatch occurs at one of the boundaries in a twin quintuplet; this twin boundary is not coherent and is called a misfit boundary. In the figure, the arrow marked A points to the beginning of a misfit twin boundary that meanders toward the periphery of the crystal. A misfit boundary can terminate within the crystallite or it can extend to the crystallite surface. Because the misfit boundary is the surface at which the crystal growth terminates locally, the local growth direction points along the boundary away from the nucleation site.

#### 2.4 Polishing CVD Diamond

CVD diamond films usually grow with surfaces that are undesirable for most optical application because of a large surface roughness. Smooth diamond films can be made if the nucleation density is high; however, the thickness of such films is limited to several micrometers as the roughness tends to increase with increasing film thickness. However, in a recent paper, Wild et al. [40] have reported that diamond films grown with a  $\langle 100 \rangle$  texture appear to grow smoother as the film thickness increases. Films of this type have been grown to thicknesses greater than  $100 \mu\text{m}$ . Transmittance measurements indicate that these films show a higher optical transmittance than conventionally grown CVD diamond films.

Methods of polishing CVD diamond films are being developed to produce smooth films. Because CVD diamond is polycrystalline and hard, it is very difficult to polish; polishing by conventional methods is very slow. Wang et al. [33] have polished CVD diamond films on a cast iron scaife heated to  $350^\circ\text{C}$ . Six weeks of polishing were required to obtain a mirror-like surface. To increase the polishing rate, a sample was annealed in an atmosphere of 0.01% oxygen in argon at  $1000^\circ\text{C}$  for 4 hours; the film surface turned black. In this case, the time for polishing was reduced to one week. Polishing with potassium nitrate also increased the polishing rate; however, the specimen had to be carefully monitored to avoid destruction. Polishing decreased the peak-to-valley surface roughness from  $1.2 \mu\text{m}$  to less than  $0.1 \mu\text{m}$ .

Yoshikawa [41] has pioneered a thermochemical method for polishing diamond at high rates. In his method, a rotating polishing plate of iron (of low carbon content) or nickel is held at an elevated temperature inside an environmental chamber capable of supporting a vacuum. The CVD diamond surface is polished by holding it in contact with the rotating plate. In an atmosphere of hydrogen, iron produced the highest polishing rate and nickel produced nearly as high a polishing rate. No polishing action was observed with molybdenum plates or with cast iron plates and no polishing was observed at  $700^\circ\text{C}$  or lower. At  $750^\circ\text{C}$  and above, the polishing rate increased with



increasing temperature. At 950 °C, the entire surface was polished after 20 min. The polishing rate also increased with applied pressure; however, excessively high pressures made the polishing process unstable. Increasing the lapping speed also increased the polishing rate. The average roughness,  $R_a$ , obtained on a 7 mm square specimen was 2.7 nm.

Frequently, the diamond surface is too rough for polishing directly. Yoshikawa has planed the surface of the specimen prior to polishing by irradiating the specimen with a Q-switched Nd-doped yttrium aluminum garnet (Nd:YAG) laser in one atmosphere of oxygen. A peak-to-valley roughness of 3  $\mu\text{m}$  could be obtained by this process. Several authors have used variations of Yoshikawa's method to polish CVD diamond [42,43]

Protrusions that sometimes grow on the diamond surface must be removed prior to polishing. Harker et al. [42] have used reactive plasma etching to remove such protrusions. In order to etch only the protrusions and not the surrounding material, a nonreactive gold coating was applied to the entire surface. The protrusions were then exposed for reactive plasma etching with oxygen.

Another method of polishing CVD diamond by ion beam polishing has been developed [44]. The rough surface of a diamond specimen is spin coated with a mixture of photoresist and a Ti-silica emulsion to produce a plane surface. The surface is then etched with an oxygen ion beam; the angle of incidence is chosen to match the etching rate of the coating with the etching rate of diamond. The average root-mean-squared roughness on a 5 cm diameter film was 4.9 nm.

## 2.5 X-ray Window

Because of its low atomic number, carbon is highly transparent to x-ray radiation. The excellent mechanical properties of diamond make it useful as an ultrathin x-ray window for an energy dispersive x-ray fluorescence detector [4]. This has been the first practical use of CVD diamond for transmitting electromagnetic radiation. In this application, diamond is replacing beryllium which must be made considerably thicker to support a vacuum. The optical transparency and mechanical stability of diamond also make CVD diamond a possible membrane material for x-ray masks. X-ray masks are used in the x-ray lithography of integrated circuits [5].

## 3. CONCLUSION

The superior properties of diamond make it a candidate for a number of optical applications. The most immediate application is the diamond x-ray window. The quality of CVD diamond for other applications, such as infrared transmissive elements and coatings, is continually improving but is not yet sufficient. Surface roughness is a major impediment to optical applications. The ability to deposit smooth surfaces would make diamond considerably more attractive as an optical material. Polishing is being pursued as a means for making smooth CVD diamond surfaces. Diamond also has promise as a blue luminescent or laser material. Identifying and controlling the relevant luminescent defect centers will be needed to improve the quantum efficiencies of such devices.

#### 4. ACKNOWLEDGEMENT

We thank J.L. Hutchison of Oxford University for his assistance in obtaining the high resolution electron micrographs.

#### 5. REFERENCES

- [1] V.P. Varnin, B.V. Deryagin, D.V. Fedoseev, I.G. Teremetskaya, and A.N. Khodan, Sov. Phys. Crystallogr. 22, 513-515 (1977).
- [2] B.V. Spitsyn, L.L. Bouilov, and B.V. Derjaguin, J. Cryst. Growth 52, 219-226 (1981).
- [3] S. Matsumoto, Y. Sato, M. Kamo, and N. Setaka, Jpn. J. Appl. Phys. 21, L183 (1982).
- [4] M.G. Peters, J.L. Knowles, M. Breen, and J. McCarthy, "Ultra-thin diamond windows for x-ray window applications," Diamond Optics II, A. Feldman and S. Holly, Editors, Proc. SPIE 1146, 217-224 (1990).
- [5] H. Windischmann and G.F. Epps, J. Appl. Phys. 68, 5665-5673 (1990).
- [6] Y. Taniguchi, K. Hirabayashi, K. Ikoma, N. Iwasaki, K. Kurihara, and M. Matsushima, Jpn. J. Appl. Phys. 28, L1848-1850 (1989).
- [7] S.C. Rand and L.G. DeShazer, Opt. Lett. 10, 481-483 (1985).
- [8] C.B. Beetz, Jr., B.A. Lincoln, and D.R. Winn, "Sub-Bandgap Excited Photoconductivity in CVD Diamond Films," Diamond Optics III, A. Feldman and S. Holly, Editors, Proc. SPIE 1325, 240-252 (1990).
- [9] W.D. Partlow, R.E. Witkowski, and J.P. McHugh in Applications of Diamond Films and Related Materials, edited by Y. Tzeng, M. Yoshikawa, M. Murakawa, and A. Feldman, Elsevier Science Publishers B.V., Amsterdam, 1991, pp. 163-168.
- [10] M. Kamo, Y. Sato, S. Matsumoto, and N. Setaka, J. Cryst. Growth 62, 642-644 (1983).
- [11] K. Suzuki, J. Yasuda, and T. Inuzuka, Appl. Phys. Lett. 50, 728-729 (1987).
- [12] S. Matsumoto, Symp. Proc. 7th International Symposium Plasma Chem., 1985, pp. 79-84.
- [13] S. Matsumoto, M. Hino, and T. Kobayashi, Appl. Phys. Lett. 51, 737-739 (1987).
- [14] Presented by A.B. Harker at the SPIE Diamond Optics IV Conference, San Diego, July 1991.
- [15] Y. Hirose and N. Kondo, Program and Book of Abstracts, Japan Applied

Physics 1988 Spring Meeting, March 29, 1988, p.434; L.M. Hanssen, W.A. Carrington, J.E. Butler, and K.A. Snail, *Materials Letters* 7, 289-292 (1991).

[16] E.N. Farabaugh, A. Feldman, and L.H. Robins, in *Applications of Diamond Films and Related Materials*, edited by Y. Tzeng, M. Yoshikawa, M. Murakawa, and A. Feldman, Elsevier Science Publishers B.V., Amsterdam, 1991, pp. 483-488.

[17] Y. Hirose, and Y. Terasawa, *Jpn. J. Appl. Phys. Part 2* 25, L519 (1986).

[18] C.-P. Chiang, D.L. Flamm, D.E. Ibbotson, and J.A. Mucha, *J. Appl. Phys.* 63, 1744-1748 (1988).

[19] e.g., D.E. Meyer, R.O. Dillon, and J.A. Woollam, in *Diamond and Diamond-Like Films*, edited by J.P. Dismukes, The Electrochemical Society, Pennington NJ, 1989, pp. 494-499.

[20] T.P. Ong and R.P.H. Chang, *Appl. Phys. Lett.* 55, 2063-2065 (1989).

[21] J.W. Glesener, A.A. Morrish, and K.A. Snail, in *Applications of Diamond Films and Related Materials*, edited by Y. Tzeng, M. Yoshikawa, M. Murakawa, and A. Feldman, Elsevier Science Publishers B.V., Amsterdam, 1991, pp. 347-351; J.W. Glesener, A.A. Morrish, and K.A. Snail, *J. Appl. Phys.*, in press.

[22] M.W. Geis, H.I. Smith, A. Argoit, J. Angus, G.-H.M. Ma, J.T. Glass, J. Butler, C.J. Robinson, and R. Pryor, *Appl. Phys. Lett.* 58, 2485-2487 (1991).

[23] J.F. Prins and H.L. Gaigher, in *New Diamond Science and Technology, Proceedings of the Second International Conference*, edited by R. Messier, J.T. Glass, J.E. Butler, and R. Roy, Materials Research Society, Pittsburgh, 1991, pp. 561-566.

[24] J. Narayan, V.P. Godbole, and C.W. White, *Science* 252, 416-418 (1991).

[25] D.E. Patterson, B.J. Bai, C.J. Chu, R.H. Hauge, and J.L. Margrave, in *New Diamond Science and Technology, Proceedings of the Second International Conference*, edited by R. Messier, J.T. Glass, J.E. Butler, and R. Roy, Materials Research Society, Pittsburgh, 1991, pp. 433-438.

[26] C. Klein, T. Hartnet, R. Miller, and C. Robinson, in *Diamond Materials, Proceedings of the Second International Symposium on Diamond Materials*, 1991, A.J. Purdes, J.C. Angus, D.F. Davis, B.M. Meyerson, K.E. Spear, and M. Yoder, Editors, The Electrochemical Society, Inc., Pennington NJ, 1991, pp.435-442.

[27] S. Musikant, *Optical Materials*, Marcel Dekker, New York and Basel, 1985, pp. 113-115.

[28] C.E. Johnson and W.A. Weimer, in *Diamond Optics II*, A. Feldman and S. Holly, Editors, *Proc. SPIE* 1146, 188-191 (1990).

[29] T. Feng, in *Diamond Optics II*, A. Feldman and S. Holly, Editors, *Proc. SPIE* 1146, 159-165 (1990).

[30] K.A. Snail, L.M. Hanssen, A.A. Morrish, and W.A. Carrington, in *Diamond*

Optics II, A. Feldman and S. Holly, Editors, Proc. SPIE 1146, 144-151 (1990).

[31] Y. Cong, R.W. Collins, G.F. Epps, and H. Windischmann, Appl. Phys. Lett. 58, 819-821 (1991).

[32] M.A. Akerman, J.R. McNeely, and R.E. Clausing, in Diamond Optics III, A. Feldman and S. Holly, Editors, Proc. SPIE 1325, 178-186 (1990).

[33] X.H. Wang, L. Pilicne, W. Zhu, W. Yarbrough, W. Drawl, and R. Messier, in Diamond Optics III, A. Feldman and S. Holly, Editors, Proc. SPIE 1325, 160-167 (1990).

[34] X.X. Bi, P.C. Eklund, J.G. Zhang, A.M. Rao, T.A. Perry, and C.P. Beetz, Jr., J. Mater. Res. 5, 811-817 (1990); X.X. Bi, P.C. Eklund, J.G. Zhang, A.M. Rao, T.A. Perry, and C.P. Beetz, Jr., in Diamond Optics II, A. Feldman and S. Holly, Editors, Proc. SPIE 1146, 192-200 (1990).

[35] A.J. Gatesman, R.H. Giles, J. Waldman, L.P. Bourget, and R. Post, in Diamond Optics III, A. Feldman and S. Holly, Editors, Proc. SPIE 1325, 170-177 (1990).

[36] E. Fritsch and D.V.G. Scarratt, in Diamond Optics II, A. Feldman and S. Holly, Editors, Proc. SPIE 1146, 201-206 (1990).

[37] L.H. Robins, E.N. Farabaugh, and A. Feldman, in Diamond Optics IV, A. Feldman and S. Holly, Editors, SPIE Proc. 1534, 105-116 (1991).

[38] L. H. Robins, L. P. Cook, E. N. Farabaugh, and A. Feldman, Phys. Rev. B, 39, 13367-13377 (1989-II).

[39] D. Shechtman, E.N. Farabaugh, L.H. Robins, A. Feldman, and J.L. Hutchison, in Diamond Optics IV, A. Feldman and S. Holly, Editors, SPIE Proc. 1534, 26-43 (1991).

[40] C. Wild, W. Muller-Sebert, T. Eckermann, and P. Koidl, in Applications of Diamond Films and Related Materials, edited by Y. Tzeng, M. Yoshikawa, M. Murakawa, and A. Feldman, Elsevier Science Publishers B.V., Amsterdam, 1991, pp. 197-205.

[41] M. Yoshikawa, in Diamond Optics III, A. Feldman and S. Holly, Editors, Proc. SPIE 1325, 210-221 (1990).

[42] A.B. Harker, J. Flintoff, J.F. and DeNatale, in Diamond Optics III, A. Feldman and S. Holly, Editors, Proc. SPIE 1325, 222-229 (1990).

[43] T.P. Thorpe, A.A. Morrish, L.M. Hanssen, J.E. Butler, and K.A. Snail, in Diamond Optics III, A. Feldman and S. Holly, Editors, Proc. SPIE 1325, 230-237 (1990).

[44] B.G. Bovard, T. Zhao, and H.A. Macleod, in Diamond Optics IV, A. Feldman and S. Holly, Editors, Proc. SPIE 1534, 216-222 (1991).

## Figure Captions

Figure 1. SEM images of diamond film surfaces exhibiting a range of morphologies. All of the films were grown at from a hydrogen-methane mixture in a hot filament CVD reactor: (upper left) "cauliflower" morphology; (upper right)  $\{110\}$  morphology; (lower left) triangular  $\{111\}$  morphology; (lower right)  $\{100\}$  morphology.

Figure 2. Infrared absorptance spectrum of a CVD diamond specimen prepared by microwave plasma CVD, courtesy of C. Klein of the Raytheon Company [26].

Figure 3. Absorption coefficients of CVD diamond films and type IIa diamond in the vicinity of the absorption edge.

Figure 4. Raman spectrum typical of CVD diamond showing a sharp diamond peak at  $1332\text{ cm}^{-1}$  and a broad diamondlike carbon peak around  $1500\text{ cm}^{-1}$ .

Figure 5. Cathodoluminescence image of diamond particles (left) and the corresponding SEM image (right).

Figure 6. Cathodoluminescence spectrum of CVD diamond film showing principal spectral features.

Figure 7. High resolution electron micrograph of CVD diamond with a  $\langle 110 \rangle$  orientation. The arrows point to misfit twin boundaries, surfaces where twins grow together noncoherently. The hollow arrows indicate local growth directions.

Figure 8. High resolution electron micrograph showing a twin quintuplet. The arrow is pointing to the start of a misfit boundary. A misfit boundary is a surface where two twins grow together noncoherently. The arrow also points in a direction of local growth.

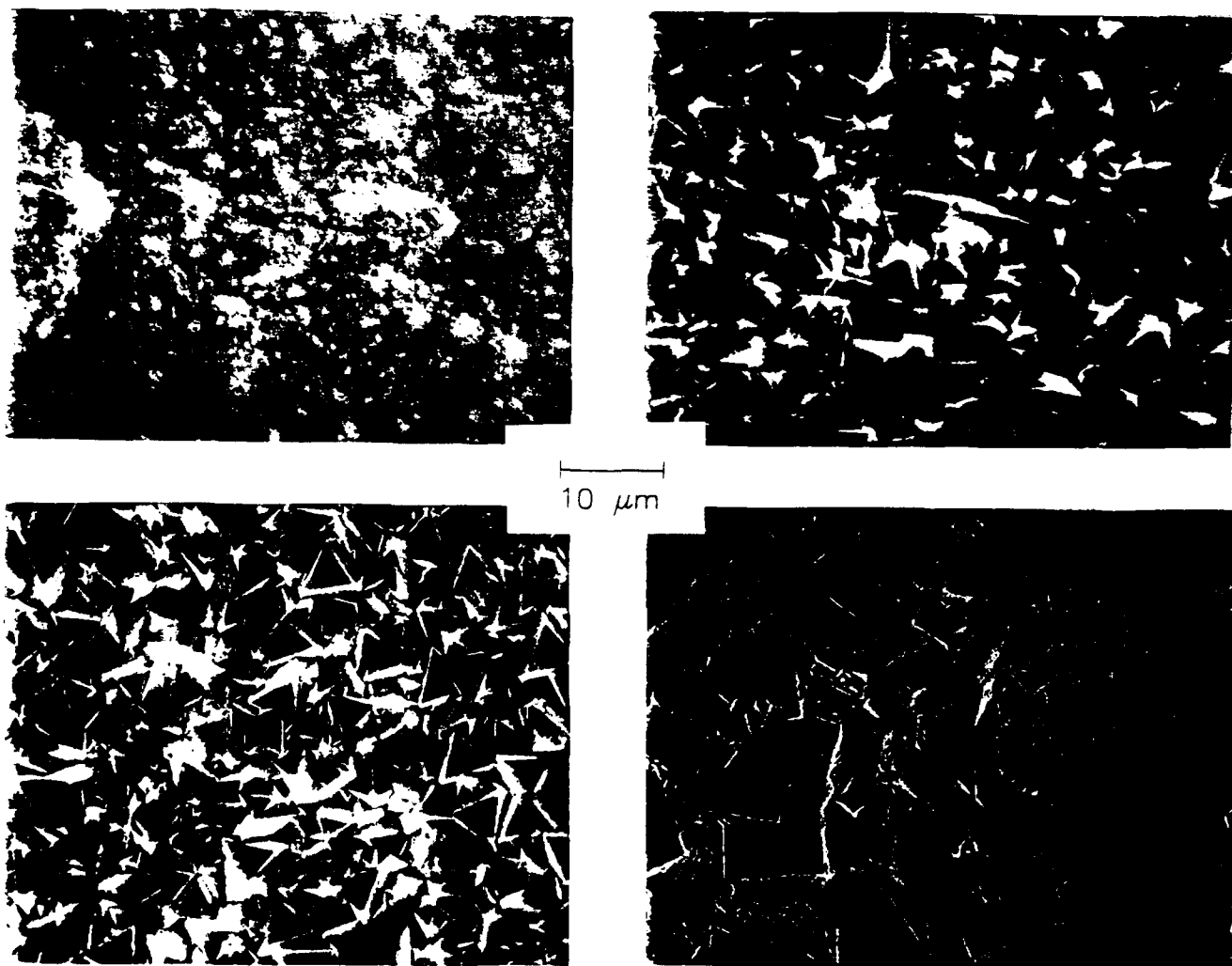


Figure 1. SEM images of diamond film surfaces exhibiting a range of morphologies. All of the films were grown at from a hydrogen-methane mixture in a hot filament CVD reactor: (upper left) "cauliflower" morphology; (upper right) {110} morphology; (lower left) triangular {111} morphology; (lower right) {100} morphology.

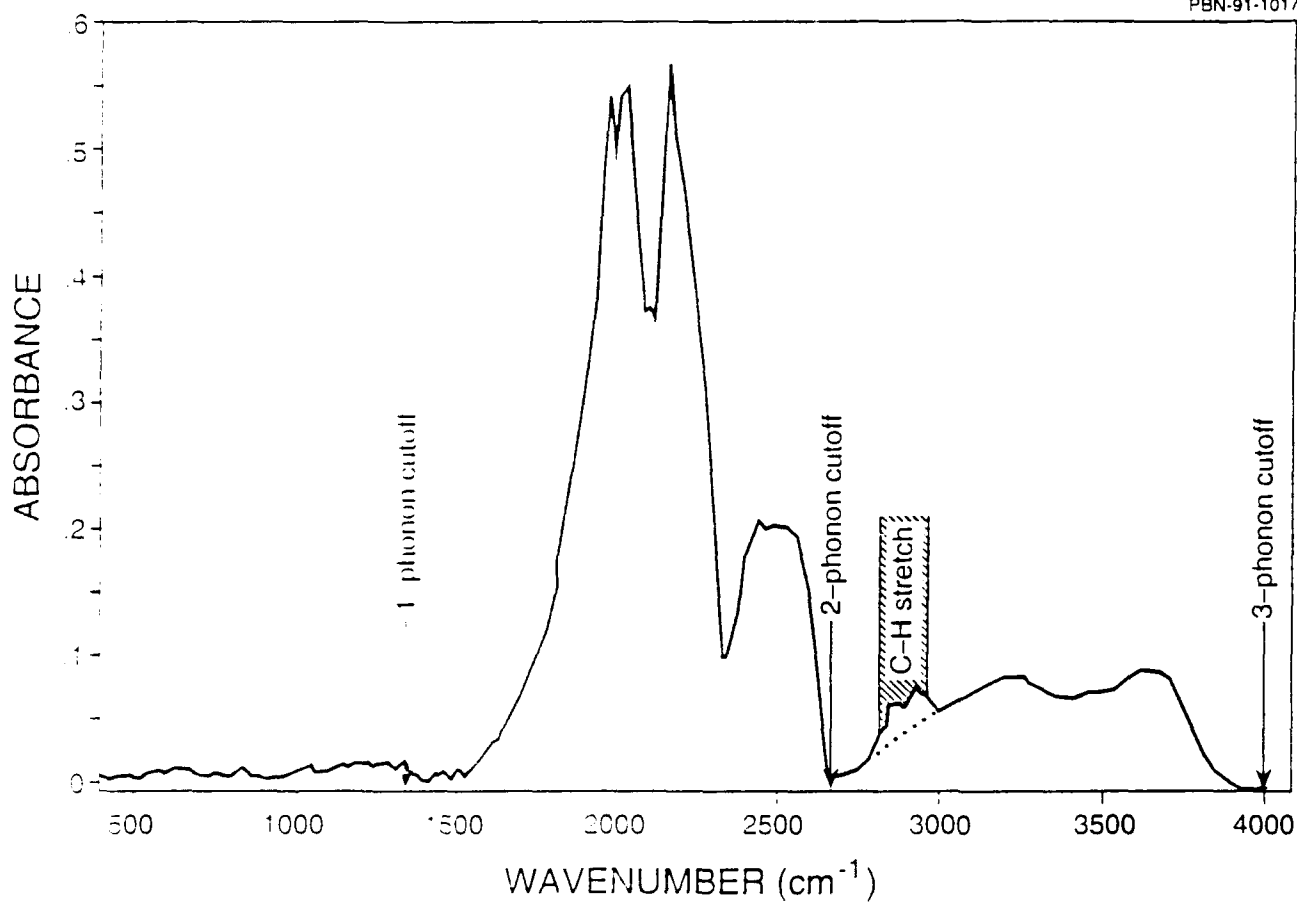


Figure 2. Infrared absorbance spectrum of a CVD diamond specimen prepared by microwave plasma CVD, courtesy of C. Klein of the Raytheon Company [26].

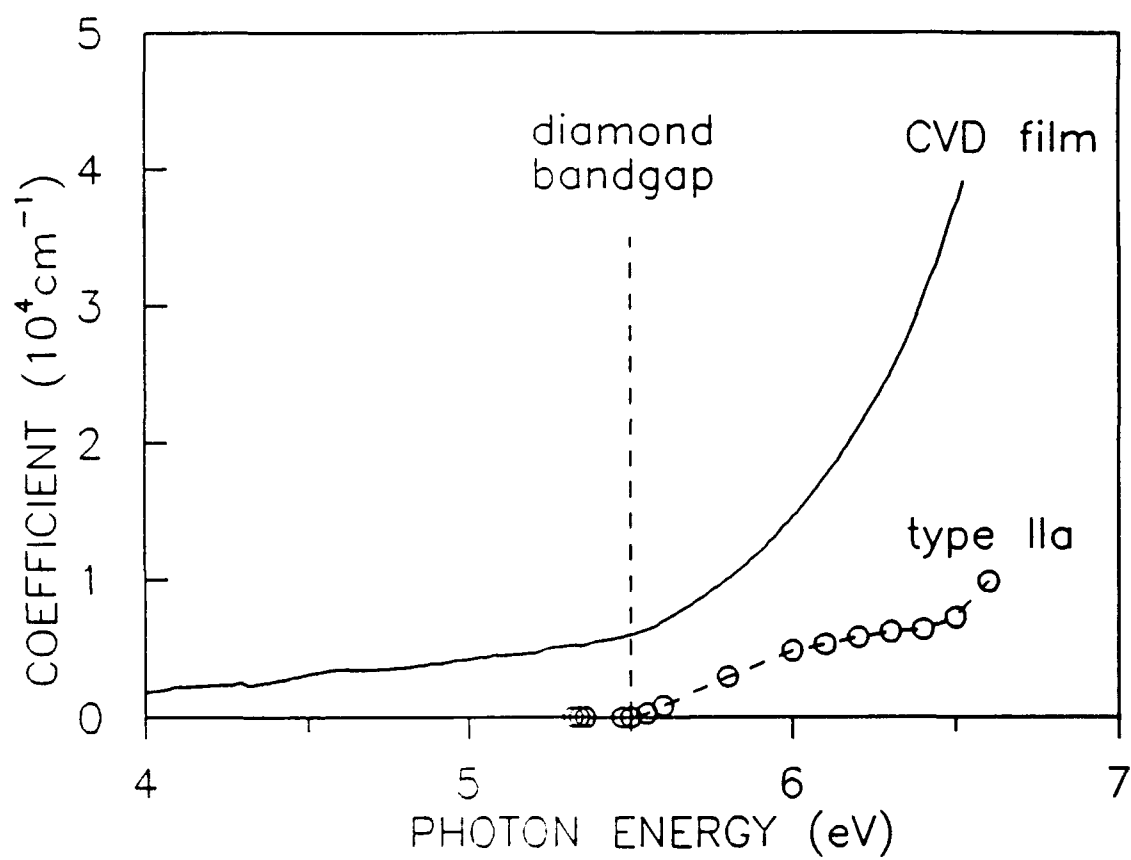


Figure 3. Absorption coefficients of a CVD diamond film and a type IIa diamond in the vicinity of the absorption edge.



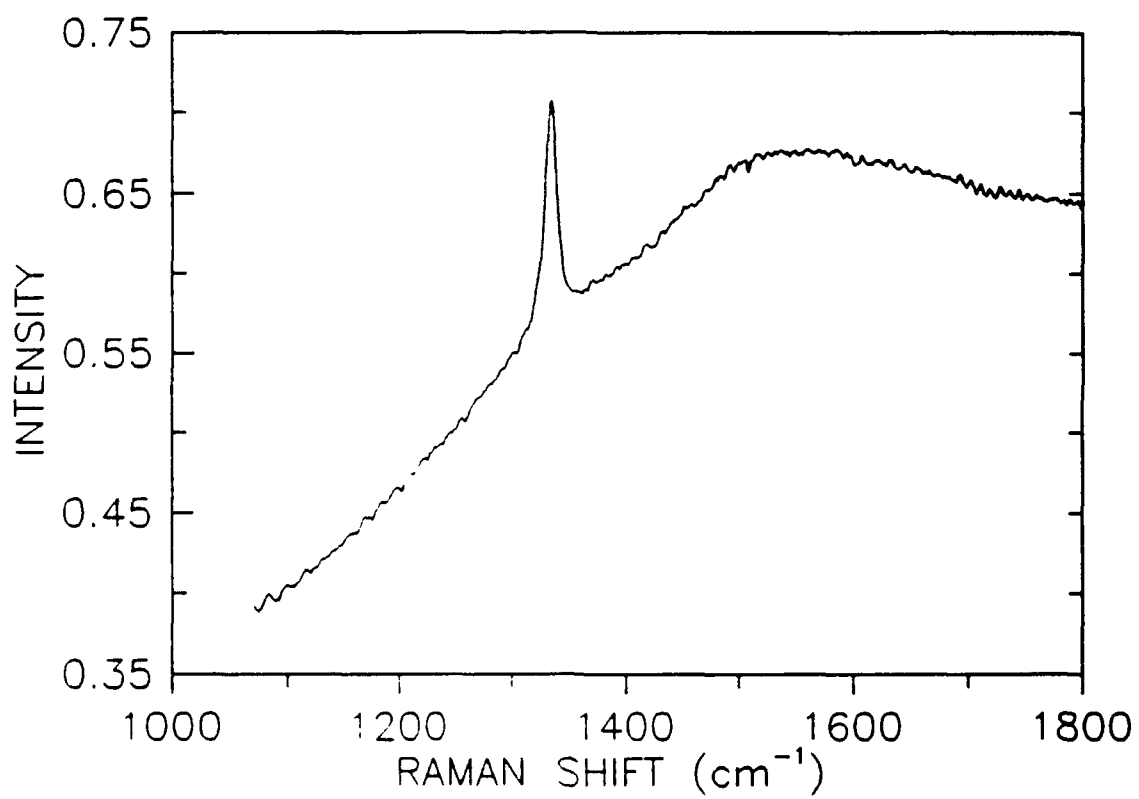


Figure 4. Raman spectrum typical of CVD diamond showing a sharp diamond peak a 1332 cm-1 and a broad diamondlike carbon peak around 1500 cm-1.



CL IMAGE



SECONDARY-ELECTRON IMAGE

Figure 5. Cathodoluminescence image of diamond particles (top) and the corresponding SEM image (bottom).

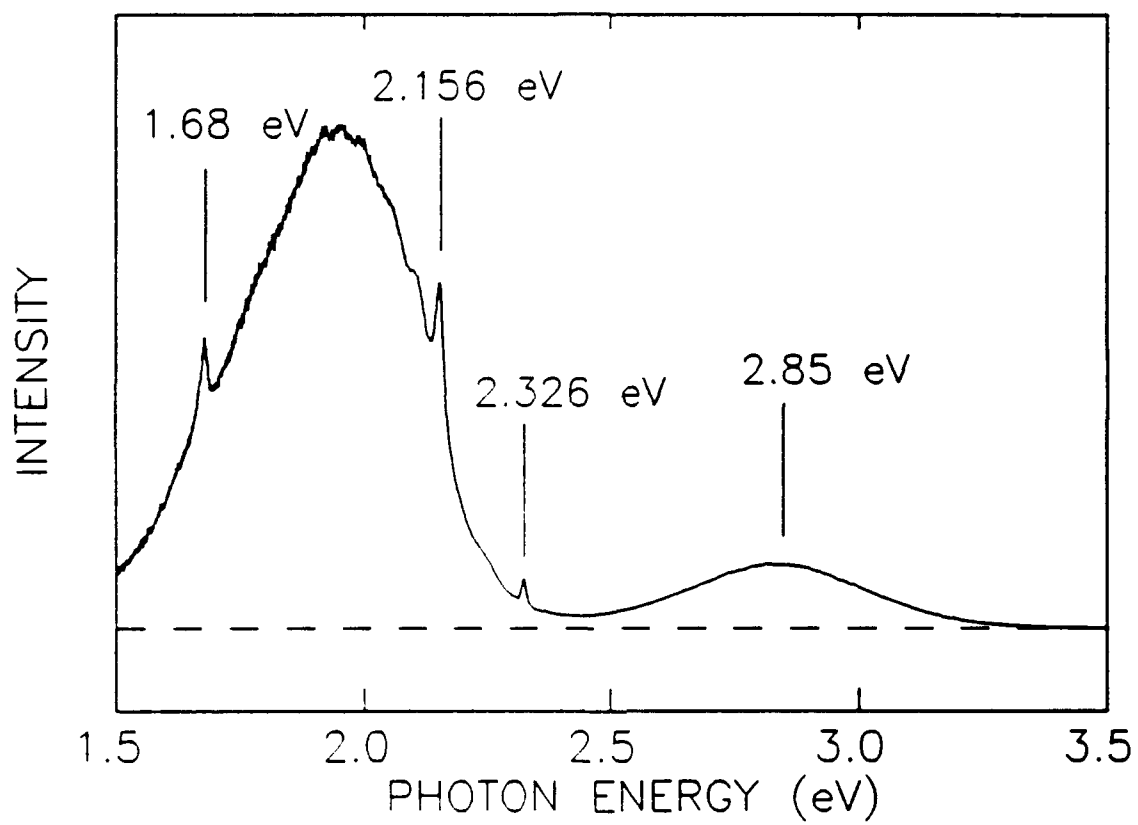


Figure 6. Cathodoluminescence spectrum of CVD diamond film showing principal spectral features.

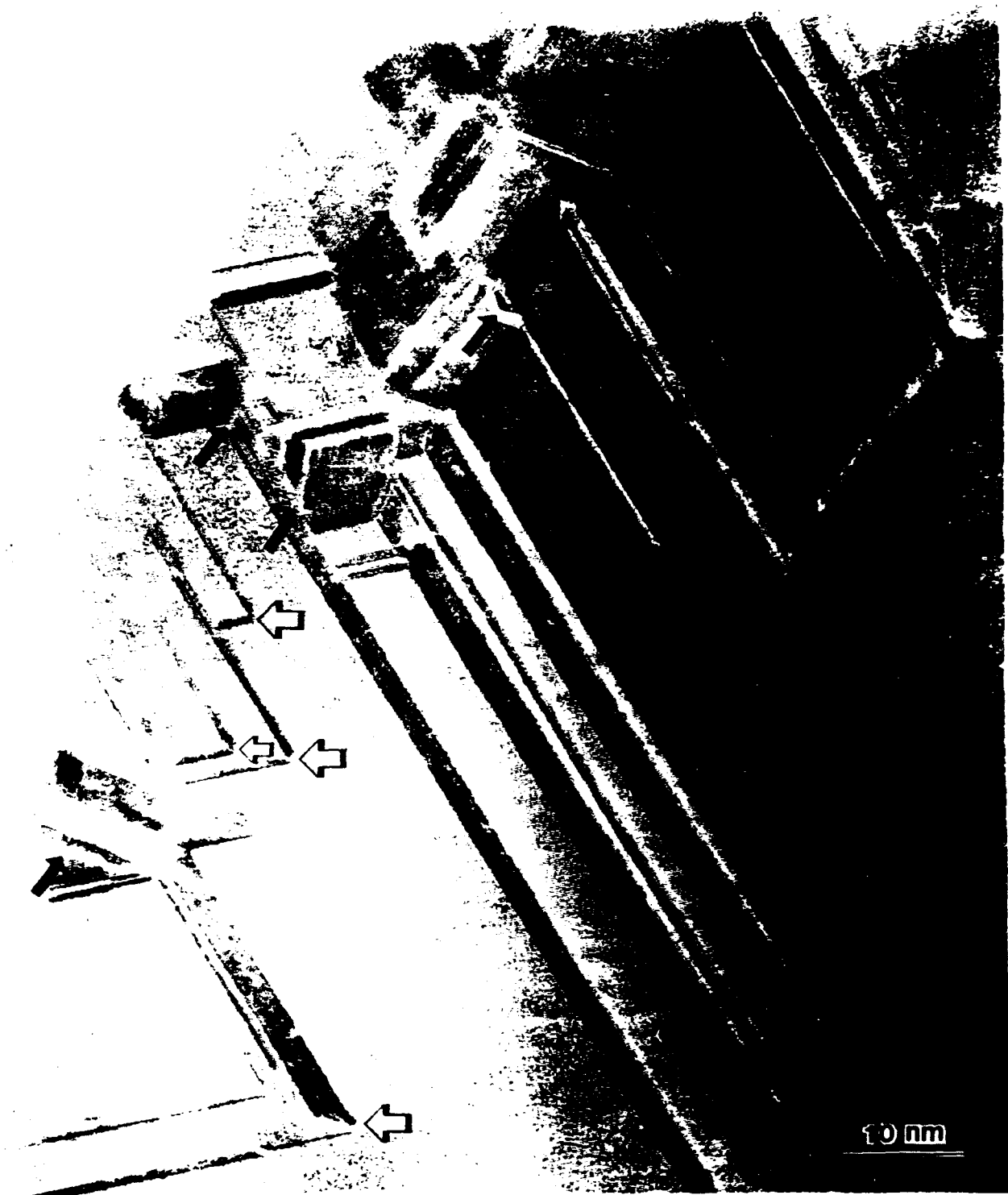


Figure 7. High resolution electron micrograph of CVD diamond with a  $\langle 110 \rangle$  orientation. The arrows point to misfit twin boundaries, surfaces where twins grow together noncoherently. The hollow arrows indicate local growth directions.

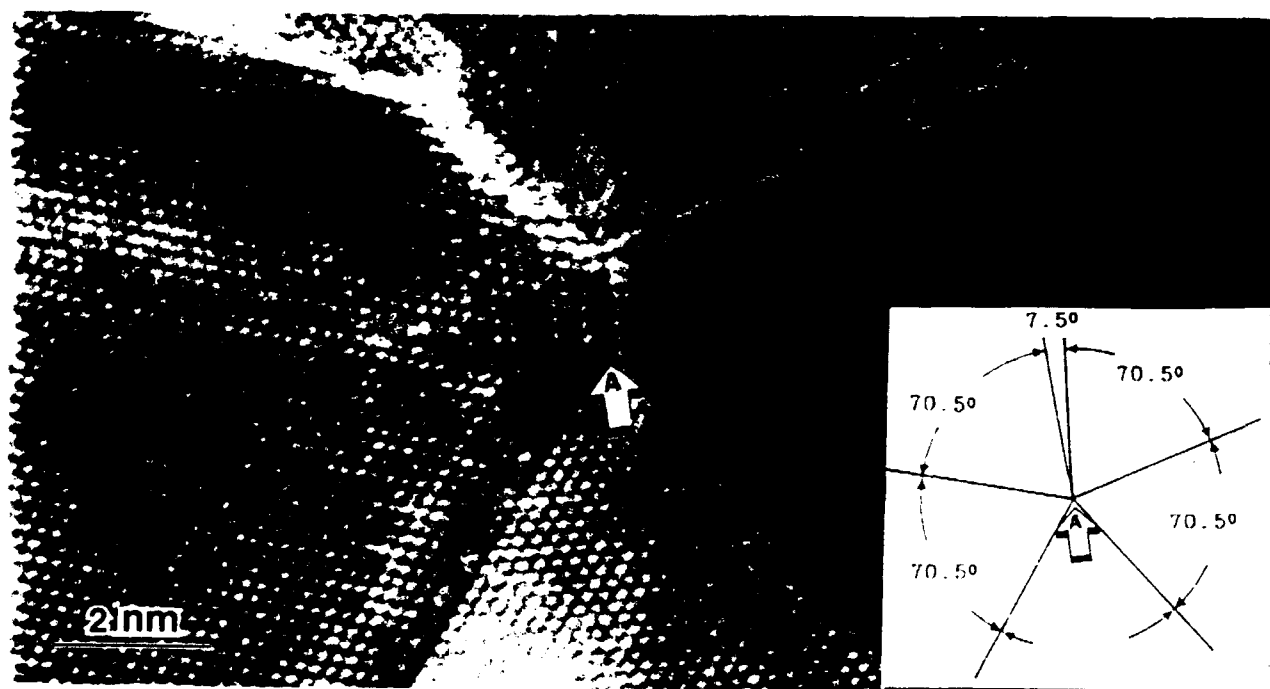


Figure 8. High resolution electron micrograph showing a twin quintuplet. The arrow is pointing to the start of a misfit boundary. A misfit boundary is a surface where two twins grow together noncoherently. The arrow also points in a direction of local growth.

FY91 ONR DOMES ARI CONTRACTORS

Dr. Duncan W. Brown  
Advanced Technology Materials, Inc.  
520-B Danbury Road  
New Milford, CT 06776  
(203) 355-2681

Dr. Mark A. Cappelli  
Stanford University  
Mechanical Engineering Dept.  
Stanford, CA 94305  
(415) 723-1745

Dr. R. P. H. Chang  
Materials Science & Engineering Dept.  
2145 Sheridan Road  
Evanston, IL 60208  
(312) 491-3598

Dr. Bruce Dunn  
UCLA  
Chemistry Department  
Los Angeles, CA 90024  
(213) 825-1519

Dr. Al Feldman  
Leader, Optical Materials Group  
Ceramics Division  
Materials Science & Engineering Lab  
NIST  
Gaithersburg, MD 20899  
(301) 975-5740

Dr. John Field  
Department of Physics  
University of Cambridge  
Cavendish Laboratory  
Madingley Road  
Cambridge CB3 0HE  
England  
44-223-337733, ext. 7318

Dr. William A. Goddard, III  
Director, Materials and Molecular  
Simulation Center  
Beckman Institute  
California Institute of Technology  
Pasadena, CA 91125  
(818) 356-6544  
Fax: (818) 568-8824

Dr. David Goodwin  
California Institute of Technology  
Mechanical Engineering Dept.  
Pasadena, CA 91125  
(818) 356-4249

Dr. Alan Harker  
Rockwell Int'l Science Center  
1049 Camino Dos Rios  
P.O. Box 1085  
Thousand Oaks, CA 91360  
(805) 373-4131

Mr. Stephen J. Harris  
General Motors Research Laboratories  
Physical Chemistry Department  
30500 Mound Road  
Warren, MI 48090-9055  
(313) 986-1305  
Fax: (313) 986-8697  
E-mail: sharris@gmr.com

Dr. Rudolph A. Heinecke  
Standard Telecommunication  
Laboratories, Ltd.  
London Road  
Harlow, Essex CM17 9MA  
England  
44-279-29531, ext. 2284

Dr. Kelvin Higa  
Code 3854  
Naval Weapons Center  
China Lake, CA 93555-6001

Dr. Curt E. Johnson  
Code 3854  
Naval Weapons Center  
China Lake, CA 93555-6001  
(619) 939-1631

Dr. J. J. Mecholsky, Jr.  
University of Florida  
Materials Science & Engineering Dept.  
256 Rhines Hall  
Gainesville, FL 32611  
(904) 392-1454

Dr. Rishi Raj  
Cornell University  
Materials Science & Engineering Dept.  
Ithaca, NY 14853  
(607) 255-4040

Dr. Rustum Roy  
Pennsylvania State University  
Materials Research Laboratory  
University Park, PA 16802  
(814) 865-2262

Dr. James A. Savage  
Royal Signals & Radar Establishment  
St. Andrews Road  
Great Malvern, Worcs WR14.3PS  
England  
01-44-684-895043

Dr. Y. T. Tzeng  
Auburn University  
Electrical Engineering Dept.  
Auburn, AL 36849  
(205) 884-1869

Dr. Terrell A. Vanderah  
Code 3854  
Naval Weapons Center  
China Lake, CA 93555-6001  
(619) 939-1654

Dr. George Walrafen  
Howard University  
Chemistry Department  
525 College Street N.W.  
Washington, D.C. 20059  
(202) 636-6897/6564

Dr. Aaron Wold  
Brown University  
Chemistry Department  
Providence, RI 02912  
(401) 863-2857

Dr. Wally Yarborough  
Pennsylvania State University  
Materials Research Laboratory  
University Park, PA 16802  
(814) 865-7102

# DISTRIBUTION LIST

Mr. James Arendt  
Hughes Aircraft Company  
8433 Fallbrook Ave. 270/072  
Canoga Park, CA 91304  
(838) 702-2890

Mr. Larry Blow  
General Dynamics  
1525 Wilson Blvd., Suite 1200  
Arlington, VA 22209  
(703) 284-9107

Mr. Ellis Boudreaux  
Code AGA  
Air Force Armament Laboratory  
Eglin AFB, FL 32542

Dr. Duncan W. Brown  
Advanced Technology Materials, Inc.  
520-B Danbury Road  
New Milford, CT 06776  
(203) 355-2681

Dr. Mark A. Cappelli  
Stanford University  
Mechanical Engineering Dept.  
Stanford, CA 94305  
(415) 723-1745

Dr. R. P. H. Chang  
Materials Science & Engineering Dept.  
2145 Sheridan Road  
Evanston, IL 60208  
(312) 491-3598

Defense Documentation Center  
Cameron Station  
Alexandria, VA 22314  
(12 copies)

Dr. Al Feldman  
Leader, Optical Materials Group  
Ceramics Division  
Materials Science & Engineering Lab  
NIST  
Gaithersburg, MD 20899  
(301) 975-5740

Dr. John Field  
Department of Physics  
University of Cambridge  
Cavendish Laboratory  
Madingley Road  
Cambridge CB3 0HE  
England  
44-223-337733, ext. 7318

Dr. William A. Goddard, III  
Director, Materials and Molecular  
Simulation Center  
Beckman Institute  
California Institute of Technology  
Pasadena, CA 91125  
(818) 356-6544  
Fax: (818) 568-8824

Dr. David Goodwin  
California Institute of Technology  
Mechanical Engineering Dept.  
Pasadena, CA 91125  
(818) 356-4249

Dr. Kevin Gray  
Norton Company  
Goddard Road  
Northboro, MA 01532  
(508) 393-5968

Mr. Gordon Griffith  
WRDC/MLPL  
Wright-Patterson AFB, OH 45433

Dr. H. Guard  
Office of Chief of Naval Research  
(ONR Code 1113PO)  
800 North Quincy Street  
Arlington, VA 22217-5000

Dr. Alan Harker  
Rockwell Int'l Science Center  
1049 Camino Dos Rios  
P.O. Box 1085  
Thousand Oaks, CA 91360  
(805) 373-4131



Mr. Stephen J. Harris  
General Motors Research Laboratories  
Physical Chemistry Department  
30500 Mound Road  
Warren, MI 48090-9055  
(313) 986-1305  
Fax: (313) 986-8697  
E-mail: sharris@gmr.com

Dr. Rudolph A. Heinecke  
Standard Telecommunication  
Laboratories, Ltd.  
London Road  
Harlow, Essex CM17 9MA  
England  
44-279-29531, ext. 2284

Dr. Curt E. Johnson  
Code 3854  
Naval Weapons Center  
China Lake, CA 93555-6001  
(619) 939-1631

Dr. Larry Kabacoff (Code R32)  
Officer in Charge  
Naval Surface Weapons Center  
White Oak Laboratory  
10901 New Hampshire  
Silver Spring, MD 20903-5000

Mr. M. Kinna  
Office of Chief of Naval Research  
(ONT Code 225)  
800 North Quincy Street  
Arlington, VA 22217-5000

Dr. Paul Klocek  
Texas Instruments  
Manager, Advanced Optical Materials Branch  
13531 North Central Expressway  
P.O. Box 655012, MS 72  
Dallas, Texas 75268  
(214) 995-6865

Ms. Carol R. Lewis  
Jet Propulsion Laboratory  
4800 Oak Grove Drive  
Mail Stop 303-308  
Pasadena, CA 91109  
(818) 354-3767

Dr. J. J. Mecholsky, Jr.  
University of Florida  
Materials Science & Engineering Dept.  
256 Rhines Hall  
Gainesville, FL 32611  
(904) 392-1454

Dr. Russ Messier  
Pennsylvania State University  
Materials Research Laboratory  
University Park, PA 16802  
(814) 865-2262

Mr. Mark Moran  
Code 3817  
Naval Weapons Center  
China Lake, CA 93555-6001

Mr. Ignacio Perez  
Code 6063  
Naval Air Development Center  
Warminster, PA 18974  
(215) 441-1681

Mr. C. Dale Perry  
U.S. Army Missile Command  
AMSMI-RD-ST-CM  
Redstone Arsenal, AL 35898-5247

Mr. Bill Phillips  
Crystallume  
125 Constitution Drive  
Menlo Park, CA 94025  
(415) 324-9681

Dr. Rishi Raj  
Cornell University  
Materials Science & Engineering Dept.  
Ithaca, NY 14853  
(607) 255-4040

Dr. M. Ross  
Office of Chief of Naval Research  
(ONR Code 1113)  
800 North Quincy Street  
Arlington, VA 22217-5000

Dr. Rustum Roy  
Pennsylvania State University  
Materials Research Laboratory  
University Park, PA 16802  
(814) 865-2262

Dr. James A. Savage  
Royal Signals & Radar Establishment  
St. Andrews Road  
Great Malvern, Worcs WR14.3PS  
England  
01-44-684-895043

Mr. David Siegel  
Office of Chief of Naval Research  
(ONT Code 213)  
800 North Quincy Street  
Arlington, VA 22217-5000

Dr. Keith Snail  
Code 6520  
Naval Research Laboratory  
Washington, D.C. 20375  
(202) 767-0390

Dr. Y. T. Tzeng  
Auburn University  
Electrical Engineering Dept.  
Auburn, AL 36849  
(205) 884-1869

Dr. George Walrafen  
Howard University  
Chemistry Department  
525 College Street N.W.  
Washington, D.C. 20054  
(202) 806-6897/6564

Mr. Roger W. Whatmore  
Plessey Research Caswell Ltd.  
Towcester Northampton NN128EQ  
England  
(0327) 54760

Dr. Charles Willingham  
Raytheon Company  
Research Division  
131 Spring Street  
Lexington, MA 02173  
(617) 860-3061

Dr. Robert E. Witkowski  
Westinghouse Electric Corporation  
1310 Beulah Road  
Pittsburgh, PA 15235  
(412) 256-1173

Dr. Aaron Wold  
Brown University  
Chemistry Department  
Providence, RI 02912  
(401) 863-2857

Mr. M. Yoder  
Office of Chief of Naval Research  
(ONR Code 1114SS)  
800 North Quincy Street  
Arlington, VA 22217-5000

Robert W. Schwartz  
Code. 38505.  
Naval Weapons Center  
China Lake, CA 93555  
619/939-1655